Clinical Neuroradiology (2024) 34:597–603
https://doi.org/10.1007/s00062-024-01399-y

ORIGINAL ARTICLE

Diagnostic Performance of Pointwise Encoding Time Reduction with Radial Acquisition Subtraction-based MR Angiography in the Follow-up of Intracranial Aneurysms after Clipping

Inyoung Kim[1] · Sung Jun Ahn[1] · Mina Park[1] · Bio Joo[1] · Junhyung Kim[2] · Sang Hyun Suh[1]

Received: 5 December 2023 / Accepted: 12 February 2024 / Published online: 8 March 2024

Abstract

Purpose While follow-up assessment of clipped aneurysms (CAs) using magnetic resonance angiography (MRA) can be challenging due to susceptibility artifacts, a novel MRA sequence pointwise encoding time reduction with radial acquisition (PETRA) subtraction-based MRA, has been developed to reduce these artifacts. The aim of the study was to validate the diagnostic performance of PETRA-MRA by comparing it with digital subtraction angiography (DSA) as a reference for follow-up of CAs using a 3T MR scanner.

Methods Patients with clipping who underwent both PETRA-MRA and DSA between September 2019 and December 2021 were retrospectively included. Two neuroradiologists independently reviewed with the reconstructed images of PETRA-MRA to assess the visibility of the arteries around the clips and aneurysm recurrence or remnants of CA using a 3-point scale. The diagnostic accuracy of PETRA-MRA was evaluated in comparison to DSA.

Results The study included 34 patients (28 females, mean age 59 ± 9.6 years) with 48 CAs. The PETRA-MRA allowed visualization of the parent vessels around the clips in 98% of cases, compared to 39% with time-of-flight (TOF) MRA ($p < 0.0001$). The DSA confirmed 14 (29.2%) residual or recurrent aneurysms. The PETRA-MRA demonstrated a high accuracy, specificity, positive predictive value, and negative predictive value of 99.2%, 100%, 100%, and 97.8%, respectively, while the sensitivity was 66.7%.

Conclusion This retrospective study demonstrates that PETRA-MRA provides excellent visibility of adjacent vessels near clips and has a high diagnostic accuracy in detecting aneurysm remnants or recurrences in CAs. Further prospective studies are warranted to establish its utility as a reliable alternative for follow-up after clipping.

Keywords Aneurysm · Clipping · Follow-up · PETRA-MRA

Introduction

The standard microsurgical procedure for treating saccular aneurysms involves ligating the aneurysm neck with a titanium clip. Although the incidence of aneurysm remnants or recurrence after clipping is low, there is substantial evidence supporting the need for routine surveillance imaging after clipping, as aneurysm recurrence or de novo aneurysm formation with subsequent subarachnoid hemorrhage (SAH) can occur [1–7]. Digital subtraction angiography (DSA) and computed tomography angiography (CTA) are the current standard of care for follow-up imaging of clipped aneurysms (CAs), but they carry the risk of radiation exposure and contrast agent toxicity [8, 9]. Time-of-flight magnetic resonance angiography (TOF-MRA) is an alternative that avoids these risks, but its use as a follow-up imaging tool is limited due to susceptibility artifacts caused by implanted clips [10]. To address these challenges, new MRA sequences with reduced susceptibility artifacts have been developed. Recent studies have shown that pointwise encoding time reduction with radial acquisition (PETRA) subtraction-based MRA (Siemens Healthineers, Erlangen,

✉ Sang Hyun Suh
suhsh11@yuhs.ac

[1] Department of Radiology, Gangnam Severance Hospital, Yonsei University College of Medicine, Seoul, Korea (Republic of)

[2] Department of Neurosurgery, Gangnam Severance Hospital, Yonsei University College of Medicine, Seoul, Korea (Republic of)

Germany) is a non-contrast MR technique like TOF-MRA and provides better visualization of adjacent vessels near implanted metals compared to TOF-MRA; however, most studies have focused only on stent-assisted coiled or simply coiled aneurysms, comparing PETRA-MRA with DSA [11–15].

Some studies [16, 17] have compared PETRA-MRA with CTA or TOF-MRA for the follow-up imaging of aneurysms after clipping, and there are a few studies of head to head comparison of PETRA-MRA and DSA as a reference for clipped aneurysms to confirm the diagnostic performance of PETRA-MRA [16, 17]. Therefore, we aimed to validate the diagnostic performance of PETRA-MRA for the follow-up imaging of CA by comparing it with DSA as a reference.

Material and Methods

Patients

The institutional review board examined this retrospective study, and the need for informed consent was waived. In our hospital, brain CTA or TOF-MRA was used as a surveillance imaging in the follow-up of CAs, while DSA was performed at the discretion of the clinician. Since September 2019, PETRA-MRA has been routinely used alongside TOF-MRA for the evaluation of CAs. Patients who underwent both PETRA-MRA and DSA within 6 months for follow-up imaging were retrospectively included from a database spanning from September 2019 to December 2021.

Exclusion criteria encompassed patients who did not undergo either PETRA-MRA or DSA, as well as those lost to follow-up. PETRA-MRA images with poor image quality due to motion artifacts were also excluded to ensure accurate comparisons.

Imaging Acquisition

Images using TOF-MRA and PETRA-MRA were acquired together in a single scan session using a 3-T MR scanner (Vida, Siemens Healthineers) with a 128-channel head-neck coil. The scan parameters for TOF-MRA were: TR/TE = 21.0/3.69 ms, flip angle = 20°, FOV = 235 × 212 mm, matrix = 384 × 344, voxel size = 0.6 × 0.6 × 0.5 mm^3, section thickness = 0.5 mm, compressed sensing factor = 9, bandwidth = 186 Hz/pixel, acquisition time = 5 min 49 s, number of slabs = 7. The following scan parameters were used for PETRA-MRA: TR/TE 5.5/0.07 ms; flip angle 6°; FOV 220 × 220 mm; matrix 256 × 256; radial sampling 33,000 radial spokes; voxel size 0.86 × 0.86 × 0.9 mm^3; slice thickness 0.9 mm; NEX 1; and bandwidth 399 Hz/pixel. Both MR sequences were performed without contrast agent. The acquisition time for PETRA-MRA was 6 min 52 s, regardless of the presence or absence of a saturation band. Maximum intensity projections were reconstructed using the system software (Siemens Healthineers). Postprocessing times for PETRA-MRA sequences was less than 5 min.

The DSA images were acquired using a biplane angiographic system (Artis zee biplane, [Siemens Healthineers, Erlangen, Germany]). In all cases, 3D rotational angiographic images were obtained following a standard protocol, and a nonionic contrast agent (Visipaque 270, [GE Healthcare Life Sciences, Buckinghamshire, UK]) was used.

Imaging Analysis

Imaging analysis was performed using the reconstructed images of both MRA and 3D images of DSA. In selected cases, the reconstructed MRA images were independently reviewed by 2 neuroradiologists (SJA and MP) with more than 10 years of experience using a picture archiving and communication system (PACS; Centricity PACS, GE Healthcare). They were blinded to all clinical information of patients except for the location of the clipped aneurysms. In cases of disagreement for evaluation of aneurysm recurrence, consensus was reached.

Visibility of the parent artery and the branch vessels near the clips in TOF-MRA and PETRA-MRA was graded by two readers using a previously published 3-point scale [16]. Aneurysm remnants or recurrence of CAs on PETRA-MRA were graded according to the following criteria. Based on the Sindou classification [18] a modified 3-point scale was used to grade aneurysm recurrence or remnant of the CAs: grade 1 was interpreted as complete clipping without recurrence, grade 2 as clipping with suspicious minimal neck, and grade 3 as clipping with definite recurrence or remnant. In addition, a dichotomized scale of absence or presence of aneurysm recurrence or remnant (grade 1 + 2 versus 3) was used.

The 3D-DSA images were graded according to the same scale by an interventional neuroradiologist (SHS) with more than 15 years of experience.

Statistical Analysis

Continuous variables were presented as mean ± standard deviation, while categorical variables were reported as frequencies and percentages. The independent 2-sample t-test was used to assess differences for continuous variables, and the χ^2-test (or Fisher's exact test) was employed for categorical variables. Interobserver agreement was evaluated using k-statistics and interpreted as follows: 0 (no agreement), 0.01–0.20 (slight agreement), 0.21–0.40 (fair agree-

ment), 0.41–0.60 (moderate agreement), 0.61–0.80 (substantial agreement), and 0.81–1.00 (almost perfect agreement) [19]. Sensitivity, specificity, accuracy, positive predictive value (PPV), and negative predictive value (NPV) of PETRA-MRA were determined using DSA as the reference for assessing aneurysm remnants or recurrence after clipping. Statistical significance was considered for *p*-values ≤ 0.05. Statistical analyses were performed using SPSS v.19.0 (IBM, Armonk, New York, USA).

Results

Patients and Aneurysm Characteristics

A total of 522 patients who underwent PETRA-MRA between September 2019 and December 2021 were initially included in this study. Among them, 470 patients without follow-up DSA were excluded. From the remaining 52 patients who had both PETRA-MRA and DSA, 18 patients were further excluded due to inadequate visibility caused by motion artifacts. Finally, a total of 34 patients (28 females) with 48 titanium alloy clipped aneurysms were included in the analysis (Table 1). The mean age of the patients was 59 ± 9.6 years. The average follow-up period between operation and subsequent MRA and DSA was 48.7 ± 47.4 months.

The average size of the aneurysms was 4.7 ± 2.2 mm in maximum diameter and 13 patients (38.2%) presented with subarachnoid hemorrhage. In terms of multiple aneurysms 11 patients (32.4%) were identified, with 9 patients having 2 aneurysms each, 1 patient with 3 aneurysms, and 1 patient with 4 aneurysms. The locations of all 48 clipped aneurysms are summarized in Table 1. The average number of clips used per aneurysm was 1.9, with a range of 1–4 clips. The number of clips used was as follows: 1 clip was required in 20, 2 in 16, 3 in 9, and 4 in 3 of the 48 aneurysms.

Visibility of the Parent and Adjacent Arteries around Clips

With PETRA-MRA, both the parent artery and the branching vessels were visible around the clip in 77.1% (37/48) of the CAs, while all vessels were visible in 29.2% (14/48) with TOF-MRA ($p < 0.0001$, Table 2). In 97.9% (47/48) of PETRA-MRA cases, the parent artery was visible around the clip, while no vessel was visible around the clip in 60.4% (29/48) of TOF-MRA cases. There was an interobserver agreement of 0.56 for the visibility of vessels with clips on PETRA-MRA.

Table 1 Demographic characteristics of 34 patients with 48 aneurysms

	Total ($n = 48$, %)
Age (years)	59 ± 9.6
Female	28 (82.4)
Aneurysmal size (mm)	
Maximum diameter	4.7 ± 2.2
Neck	3.4 ± 1.3
SAH	13 (38.2)
Multiplicity[a]	11 (32.4)
Aneurysm location	
ICA	19 (38.8)
Distal ICA	12 (24.5)
Cavernous ICA	4 (8.2)
ICA bifurcation	3 (6.1)
MCA	18 (37.5)
M1 (sphenoid)	1 (2.0)
MCBIF	16 (33.3)
M2 (insular)	1 (2.0)
ACA	10 (20.4)
Acom	9 (18.4)
A2 and A3	1 (2.04)
BA	1 (2.04)
Clips used	
1	20 (41.7)
2	16 (33.3)
3	9 (18.8)
4	3 (6.3)

n number, *ICA* intracranial artery, *MCBIF* middle cerebral artery bifurcation, *BA* basilar artery; *ACA* anterior cerebral artery, *MCA* middle cerebral artery, *Acom* anterior communicating artery, *SAH* subarachnoid hemorrhage

[a]2 aneurysms in 9 patients, 3 aneurysms in 1 patient, 4 aneurysms in 1 patient

Diagnostic Performance of PETRA-MRA for Detection of Aneurysm Remnants or Recurrence

Of the 48 CAs, a total of 14 (29.2%) cases were confirmed as grade 2 or 3 by DSA (Table 3). The mean size of the residual aneurysm was 1.58 ± 0.72 mm, for the 11 cases diagnosed as grade 2 by DSA it was 1.3 ± 0.4 mm and the remaining 3 cases diagnosed as grade 3 were 2.5 ± 0.7 mm ($p = 0.0018$). Of the 14 cases, 9 cases interpreted as grade 1 on PETRA-MRA were less than 2 mm in size and 5 cases interpreted as grade 2 or 3 were equal to or greater than 2 mm.

For the detection of aneurysm recurrence or remnants, PETRA-MRA showed an accuracy of 99.2%, sensitivity of 66.7%, specificity of 100%, PPV of 100%, and NPV of 97.8%.

The interobserver agreement between the two readers for PETRA-MRA was 0.45 on a 3-point scale and 0.68 on the dichotomized scale. On a 3-point scale, 9 out of 48 cases

Table 2 Comparison between TOF-MRA and PETRA-MRA for visibility of the parent artery and adjacent arteries near the clip

Arterial visibility near the clip ($n=48$)	TOF-MRA (%)	PETRA-MRA (%)	p-value
No signal from all vessels	29 (60.4)	1 (2.1)	<0.0001
Visible parent artery but no signal from any other distal vessels	5 (10.4)	10 (20.8)	0.16
All vessels visible	14 (29.2)	37 (77.1)	<0.0001

Table 3 Characteristics of 14 patients with aneurysm remnants or recurrence confirmed by DSA

No	Location	Size of aneurysm remnant or recurrence (mm)	No. of clips	Consensus reading[a]	
				PETRA-MRA	DSA
1	MCBIF	2	4	2	2
2	Distal ICA	1	1	1	2
3	Distal ICA	1.7	1	1	3
4	Cavernous ICA	1	1	1	2
5	BA	1	2	1	2
6	Cavernous ICA	1	1	1	2
7	Cavernous ICA	1	2	1	2
8	Distal ICA	2	1	2	2
9	Distal ICA	2	2	2	2
10	MCBIF	2.9	2	3	3
11	Distal ICA	1	2	1	2
12	MCBIF	1.5	3	1	2
13	MCBIF	3	2	3	3
14	Acom	1	2	1	2

No number, *ICA* intracranial artery, *Acom* anterior communicating artery, *MCBIF* middle cerebral artery bifurcation, *BA* basilar artery
[a]1 = clipping without recurrence, 2 = clipping with suspicious aneurysm neck, 3 = clipping with definite aneurysm neck or recurrence

Table 4 Reading between PETRA-MRA and DSA using a 3-grade scale

	DSA			
PETRA-MRA	1	2	3	Total
1	**34**	*8*	*1*	43
2	0	**3**	0	3
3	0	0	**2**	2
Total	34	11	3	48

The numbers in bold indicate cases of agreement between DSA and PETRA-MRA, while the numbers in italics indicate cases of disagreement
1 complete clipping without recurrence, *2* clipping with suspicious aneurysm neck, *3* clipping with definite aneurysm neck or recurrence

(18.8%) showed discordance (Table 4). Of these cases, 8 were interpreted as grade 1 on PETRA-MRA and grade 2 on DSA. The remaining false negative case was interpreted as grade 1 on PETRA-MRA and grade 3 on DSA, which also showed discordance on the dichotomized scale (Fig. 1).

Discussion

In this study, we demonstrated that PETRA-MRA showed an excellent diagnostic performance in detecting aneurysm remnants or recurrence for CAs, with good visibility of the neighboring vessels near the clips, which demonstrated specificity, PPV, NPV, and accuracy rates exceeding 99%, along with a moderate sensitivity. The interobserver agreement of PETRA-MRA readings was moderate on a 3-point scale and substantial on the dichotomized scale. The low interobserver agreement on the 3-point scale may be due to (1) the diagnostic power of PETRA is likely limited by aneurysm size, and aneurysm remnants smaller than 2 mm in PETRA were not diagnosed as described in this study and (2) the diagnostic criteria for a grade 2 suspicious neck remnant may be ambiguous for the 2 readers for PETRA.

While DSA and CTA are currently the standard of care for follow-up imaging of CAs, TOF-MRA is commonly used as a screening tool for unruptured cerebral aneurysms [8, 20]. Recently, new ultra-short echo time MR sequences such as PETRA-MRA and Silent MRA (GE Healthcare, Milwaukee, USA) have been developed to improve image quality by reducing metal artifacts, highlighting the advantages of MRA [21, 22]. Moreover, PETRA-MRA provided superior visualization of aneurysms with decreased flow dephasing and increased edge sharpness compared to TOF-MRA, which was primarily attributed to suppression of the background tissue and venous flow [23, 24]. Several preliminary studies have been published on the clinical appli-

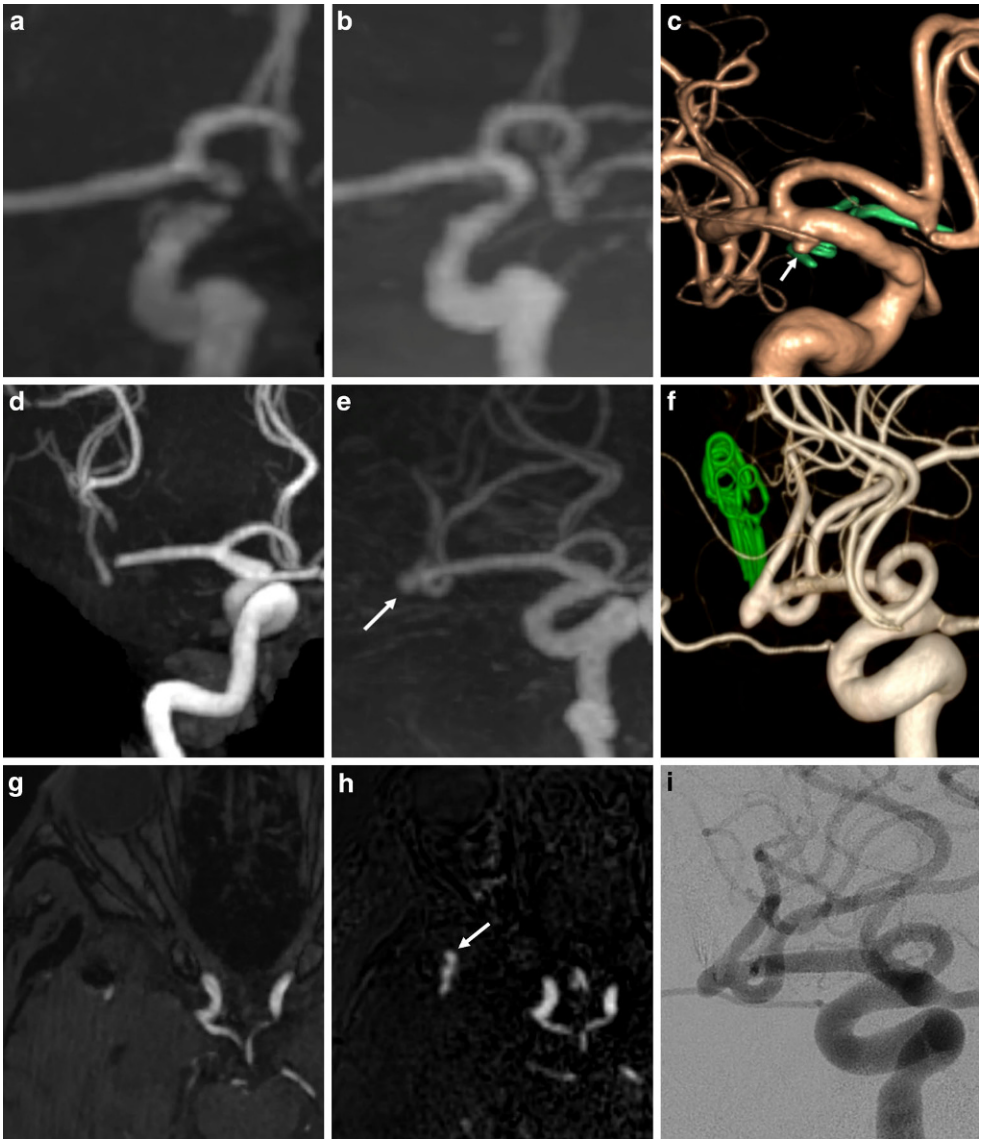

Fig. 1 False negative (*top row*) and true positive (*middle and bottom rows*) cases; TOF-MRA (**a**, **d**), PETRA-MRA (**b**, **e**), 3D-DSA (**c**, **f**) and source image of TOF-MRA (**g**), PETRA-MRA (**h**) and DSA (**i**). In the false negative case (*top row*), PETRA-MRA showed complete clipping but 3D-DSA confirmed the presence of a 2 mm aneurysm remnant (*arrow*). Note that the anterior choroidal artery was not visualized on PETRA-MRA. In the *middle and bottom rows*, both PETRA-MRA (*arrow*) and DSA readings were consistent and showed a definite aneurysm recurrence or remnant which was larger than 2 mm

cation of PETRA-MRA to reduce metal artifacts in CAs and to identify signals in the vessels around the clip [16, 17, 25]. This study is the first to validate the diagnostic accuracy of PETRA-MRA by head to head comparison with DSA and to determine whether this MRA sequence can be used as an alternative imaging modality for the follow-up of CA.

Van Loon et al. [26] reported that CTA was superior to MRA in aneurysms with titanium clips, and they recommended CTA as the preferred imaging modality for routine surveillance. Kim et al. [27] found that the sensitivity of CTA in detecting residual and recurrent aneurysms was 79–83% compared to 3D DSA; however, CTA is generally less accurate than DSA, particularly for small aneurysms (<2 mm), cases with multiple or cobalt alloy clips, aneurysms located on small parent vessels or those near bony structures [27–29]. Xiang et al. [30] suggested that the sensitivity and specificity of TOF-MRA in detecting the aneurysm remnants after clipping were 50.0% and 100%, respectively. They observed that the artifacts in TOF-MRA prevented the detection of the small residual neck in 3 CAs as visualized on DSA. In our study, PETRA-MRA demonstrated a sensitivity of 66.7% and specificity of 100% in detecting aneurysm recurrence or remnants after clipping, which were higher than those of TOF-MRA.

Our study demonstrated that approximately 78% of the cases had excellent visibility of all adjacent vessels near the clips, and more than 95% of the parent vessels were visible, which is superior to previous studies. Some authors have suggested that approximately 84% of the parent arteries around clips were visible on PETRA-MRA or Silent MRA [16, 25]. Moreover, previous studies have reported lower visibility rates for all neighboring vessels near the clips, ranging from 53% to 69% compared to this study [16, 17].

In this study, most of the parent arteries around the clips are visible, making it easier to evaluate remnants or recurrence of the peri-clip lesion; however, the branching vessels distal to the clips were not visible in 10 cases, with 50% of those cases treated with more than 3 clips. Also PETRA-MRA could be influenced by factors such as the number of clips used and the orientation of the clips relative to the magnetic field [16, 31].

Of 14 positive lesions on DSA, the size of the aneurysm remnant or recurrence was less than 2 mm in 9 discordant cases, which were interpreted as grade 1 on PETRA-MRA by a 3-point scale. Of these discordant cases, 8 cases were interpreted as grade 2 on DSA and 1 case as grade 3, which was a clipped aneurysm involving the anterior choroidal artery (Fig. 1). In the 5 concordant cases the aneurysms were larger than 2 mm. Notably, two CAs of more than 2.5 mm were initially suspected of being aneurysm recurrences on PETRA-MRA, which was located in the bifurcation of the middle cerebral artery. Although the size of the residual aneurysm may be an important factor in the diagnostic performance of PETRA-MRA [32] it is important that aneurysm recurrence or remnants larger than 2 mm can be diagnosed with PETRA-MRA in clipped aneurysms.

Limitations

Our study has several limitations that should be considered. First, it had a retrospective design, which introduces the possibility of selection bias. Although we had many PETRA-MRA cases during the study period (more than 500), only a limited number of cases could be included in this study due to the lack of follow-up DSA and inconsistent intervals between DSA and PETRA-MRA, leading to a potential selection bias. Second, approximately 30% of the 52 subjects in this study were excluded due to poor image acquisition caused by motion artifacts, especially in the early stages of implementation of the new MR sequence with its longer scan time. In general, TOF-MRA has better image quality than PETRA-MRA [16], and to improve the background noise and the low signal-to-noise ratio in PETRA-MRA You et al. [33] have proposed the use of a deep learning model. Third, it was difficult to differentiate between an aneurysm remnant and a recurrent aneurysm, which may occur in CAs during the 48-month follow-up period. Furthermore, this would require a review of the operative records, which unfortunately was not included in this study; however, two aneurysms larger than 2.5 mm were diagnosed as recurrences and treated with coil embolization.

Conclusion

This retrospective study demonstrates that PETRA-MRA provides good visibility of adjacent vessels near the clips and high diagnostic accuracy in detecting aneurysm remnants or recurrence in CAs. These results suggest that PETRA-MRA may be a valuable imaging tool for the surveillance and follow-up of CAs; however, further studies are needed to validate these findings in a prospective large cohort study, which will strengthen PETRA-MRA as a reliable alternative to other imaging modalities for the follow-up after clipping.

Author Contribution I. Kim: material preparation, data collection and analysis, writing of the first draft of the manuscript; S.J. Ahn: material preparation, data collection and analysis. M. Park: material preparation, data collection and analysis. B. Joo: material preparation, data collection and analysis. J. Kim: material preparation, data collection and analysis. S.H. Suh: material preparation, data collection and analysis, writing of the first draft of the manuscript. All authors contributed to the study's conception and design. All authors commented on previous versions of the manuscript. All authors read and approved the final manuscript.

Declarations

Conflict of interest I. Kim, S.J. Ahn, M. Park, B. Joo, J. Kim and S.H. Suh declare that they have no competing interests.

Ethical standards For this article no studies with human participants or animals were performed by any of the authors. All studies mentioned were in accordance with the ethical standards indicated in each case. The ethics approval (3-2022-0486) was obtained from the institutional review board of Gangnam Severance Hospital and the informed consent was waived.

References

1. Lin T, Fox AJ, Drake CG. Regrowth of aneurysm sacs from residual neck following aneurysm clipping. J Neurosurg. 1989;70:556–60.
2. Tsutsumi K, Ueki K, Usui M, Kwak S, Kirino T. Risk of recurrent subarachnoid hemorrhage after complete obliteration of cerebral aneurysms. Stroke. 1998;29:2511–3.
3. David CA, Vishteh AG, Spetzler RF, Lemole M, Lawton MT, Partovi S. Late angiographic follow-up review of surgically treated aneurysms. J Neurosurg. 1999;91:396–401.
4. Juvela S. Risk of subarachnoid hemorrhage from a de novo aneurysm. Stroke. 2001;32:1933–4.
5. Tsutsumi K, Ueki K, Morita A, Usui M, Kirino T. Risk of aneurysm recurrence in patients with clipped cerebral aneurysms: results of long-term follow-up angiography. Stroke. 2001;32:1191–4.
6. van der Schaaf IC, Velthuis BK, Wermer MJ, Majoie C, Witkamp T, de Kort G, Freling NJ, Rinkel GJ, Group AS. New detected aneurysms on follow-up screening in patients with previously clipped intracranial aneurysms. comparison with DSA or CTA at the time of SAH. Stroke. 2005;36:1753–8.
7. Wermer MJ, van der Schaaf IC, Velthuis BK, Algra A, Buskens E, Rinkel GJ, Group AS. Follow-up screening after subarachnoid haemorrhage. frequency and determinants of new aneurysms and enlargement of existing aneurysms. Brain. 2005;128:2421–9.

8. Wallace RC, Karis JP, Partovi S, Fiorella D. Noninvasive imaging of treated cerebral aneurysms, Part II: CT angiographic follow-up of surgically clipped aneurysms. AJNR Am J Neuroradiol. 2007;28:1207–12.
9. Kaufmann TJ, Huston J 3rd, Mandrekar JN, Schleck CD, Thielen KR, Kallmes DF. Complications of diagnostic cerebral angiography: evaluation of 19,826 consecutive patients. Radiology. 2007;243:812–9.
10. Jager HR, Mansmann U, Hausmann O, Partzsch U, Moseley IF, Taylor WJ. MRA versus digital subtraction angiography in acute subarachnoid haemorrhage: a blinded multireader study of prospectively recruited patients. Neuroradiology. 2000;42:313–26.
11. Heo YJ, Jeong HW, Baek JW, Kim ST, Jeong YG, Lee JY, Jin SC. Pointwise Encoding Time Reduction with Radial Acquisition with Subtraction-Based MRA during the Follow-Up of Stent-Assisted Coil Embolization of Anterior Circulation Aneurysms. Ajnr Am J Neuroradiol. 2019;40:815–9.
12. You SH, Kim B, Yang KS, Kim BK, Ryu J. Ultrashort Echo Time Magnetic Resonance Angiography in Follow-up of Intracranial Aneurysms Treated With Endovascular Coiling: Comparison of Time-of-Flight, Pointwise Encoding Time Reduction With Radial Acquisition, and Contrast-Enhanced Magnetic Resonance Angiography. Neurosurgery. 2021;88:E179–e89.
13. Heo YJ, Jeong HW, Kim D, Baek JW, Han JY, Choo HJ, Kim ST, Jeong YG, Jin SC. Usefulness of pointwise encoding time reduction with radial acquisition sequence in subtraction-based magnetic resonance angiography for follow-up of the Neuroform Atlas stent-assisted coil embolization for cerebral aneurysms. Acta Radiol. 2021;62:1193–9.
14. Ebiko Y, Wakabayashi H, Okada T, Mizoue T, Wakabayashi S. Usefulness of PETRA-MRA for Postoperative Follow-Up of Stent-Assisted Coil Embolization of Cerebral Aneurysms. J Neuroendovasc Ther. 2023;17:188–95.
15. Sato K, Asano A, Kobayashi T, Aoki H, Jinguji S, Seto H, Demachi H, Hasegawa H, Fujii Y. Validity of PETRA-MRA for Stent-Assisted Coil Embolization of Intracranial Aneurysms. J Neuroendovasc Ther. 2021;15:352–9.
16. Kim JH, Ahn SJ, Park M, Kim YB, Joo B, Lee W, Suh SH. Follow-up imaging of clipped intracranial aneurysms with 3-T MRI: comparison between 3D time-of-flight MR angiography and pointwise encoding time reduction with radial acquisition subtraction-based MR angiography. J Neurosurg. 2021; https://doi.org/10.3171/2021.7.JNS211197.1-6.
17. Nishikawa A, Kakizawa Y, Wada N, Yamamoto Y, Katsuki M, Uchiyama T. Usefulness of Pointwise Encoding Time Reduction with Radial Acquisition and Subtraction-Based Magnetic Resonance Angiography after Cerebral Aneurysm Clipping. World Neurosurg. 2021;X(9):100096.
18. Sindou M, Acevedo JC, Turjman F. Aneurysmal remnants after microsurgical clipping: classification and results from a prospective angiographic study (in a consecutive series of 305 operated intracranial aneurysms). Acta Neurochir (wien). 1998;140:1153–9.
19. Landis JR, Koch GG. The measurement of observer agreement for categorical data. Biometrics. 1977;33:159–74.
20. Kim JH, Lee KY, Ha SW, Suh SH. Prevalence of Unruptured Intracranial Aneurysms: A Single Center Experience Using 3T Brain MR Angiography. Neurointervention. 2021;16:117–21.
21. Gruwel MLH, Latta P, Wojna-Pelczar A, Wolfsberger S, Tomanek B. MR imaging of tissue near aneurysm clips using short- and zero time MR sequences. Measurement. 2018;130:398–403.
22. Holdsworth SJ, Macpherson SJ, Yeom KW, Wintermark M, Zaharchuk G. Clinical Evaluation of Silent T1-Weighted MRI and Silent MR Angiography of the Brain. AJR Am J Roentgenol. 2018;210:404–11.
23. Fu Q, Zhang XY, Deng XB, Liu DX. Clinical evaluation of subtracted pointwise encoding time reduction with radial acquisition-based magnetic resonance angiography compared to 3D time-of-flight magnetic resonance angiography for improved flow dephasing at 3 Tesla. Magn Reson Imaging. 2020;73:104–10.
24. Grodzki DM, Jakob PM, Heismann B. Ultrashort echo time imaging using pointwise encoding time reduction with radial acquisition (PETRA). Magn Reson Med. 2012;67:510–8.
25. Katsuki M, Narita N, Ishida N, Sugawara K, Watanabe O, Ozaki D, Sato Y, Kato Y, Jia W, Tominaga T. Usefulness of 3 Tesla Ultrashort Echo Time Magnetic Resonance Angiography (UTE-MRA, SILENT-MRA) for Evaluation of the Mother Vessel after Cerebral Aneurysm Clipping: Case Series of 19 Patients. Neurol Med Chir (tokyo). 2021;61:193–203.
26. van Loon JJ, Yousry TA, Fink U, Seelos KC, Reulen HJ, Steiger HJ. Postoperative spiral computed tomography and magnetic resonance angiography after aneurysm clipping with titanium clips. Neurosurgery. 1997;41:851–6. discussion 6–7.
27. Kim HJ, Yoon DY, Kim ES, Yun EJ, Jeon HJ, Lee JY, Cho BM. 256-row multislice CT angiography in the postoperative evaluation of cerebral aneurysms treated with titanium clips: using three-dimensional rotational angiography as the standard of reference. Eur Radiol. 2020;30:2152–60.
28. Sagara Y, Kiyosue H, Hori Y, Sainoo M, Nagatomi H, Mori H. Limitations of three-dimensional reconstructed computerized tomography angiography after clip placement for intracranial aneurysms. J Neurosurg. 2005;103:656–61.
29. Dehdashti AR, Binaghi S, Uske A, Regli L. Comparison of multislice computerized tomography angiography and digital subtraction angiography in the postoperative evaluation of patients with clipped aneurysms. J Neurosurg. 2006;104:395–403.
30. Xiang S, Fan F, Hu P, Yang K, Zhai X, Geng J, Ji Z, Lu J, Zhang H. The sensitivity and specificity of TOF-MRA compared with DSA in the follow-up of treated intracranial aneurysms. J Neurointerv Surg. 2021;13:1172–9.
31. Guermazi A, Miaux Y, Zaim S, Peterfy CG, White D, Genant HK. Metallic artefacts in MR imaging: effects of main field orientation and strength. Clin Radiol. 2003;58:322–8.
32. Li MH, Li YD, Tan HQ, Gu BX, Chen YC, Wang W, Chen SW, Hu DJ. Contrast-free MRA at 3.0 T for the detection of intracranial aneurysms. Neurology. 2011;77:667–76.
33. You SH, Cho Y, Kim B, Yang KS, Kim BK, Park SE. Synthetic Time of Flight Magnetic Resonance Angiography Generation Model Based on Cycle-Consistent Generative Adversarial Network Using PETRA-MRA in the Patients With Treated Intracranial Aneurysm. J Magn Reson Imaging. 2022;56:1513–28.